

Supplementary information

FMRI network dynamics underpinning the impact of affective carryover on cognitive control

Julian Gaviria ^{*a,b,c}. ORCID ID: 0000-0002-4266-1371

Gwladys Rey ^d. ORCID ID: 0000-0001-7192-1577

Matt L. Miller ^e. ORCID ID: 0000-0002-2377-6325

Thomas Bolton^f. ORCID ID: 0000-0002-2081-4031

Dimitri Van De Ville ^{g, h}. ORCID ID: 0000-0002-2879-3861

Patrik Vuilleumierⁱ. ORCID ID: 0000-0002-8198-9214

Authors

^aDepartment of Psychiatry, Amsterdam UMC; ^bAmsterdam Neuroscience, Amsterdam UMC; ^cVrije Universiteit, Amsterdam, The Netherlands; ^dMaster of Advanced Studies (MAS) in Neuropsychology, University of Geneva, Switzerland; ^eREACH Institute, Arizona State University, USA; ^fdepartment of Psychiatry, University of Geneva, Switzerland; ^gMedical image processing lab, Neuro-X Institute, Ecole polytechnique fédérale de Lausanne (EPFL), Switzerland; ^hDepartment of radiology and medical informatics, University of Geneva, Switzerland. ⁱLaboratory for behavioral neurology and Imaging of cognition, University of Geneva, Switzerland.

*Correspondence

Julian Gaviria. E-mail: jualgalo@gmail.com;

Keywords

Brain networks; emotions; dynamic functional connectivity (dFC); Task-rest association. Cognitive control

Contents

Supplementary methods.....	3
Experimental data.....	3
Affective stimuli	3
Subjective emotional measurements.....	4
Cognitive control task.....	4
fMRI data acquisition	6
GLM-based fMRI analysis	6
Preprocessing for co-activation pattern (CAP) analysis	7
Bayesian structural equation modelling (BSEM)	7
BSEM specification	7
BSEM model validation tests and invariance.....	8
Model convergence assessment.....	9
Supplementary results.....	10
Behavioral indices of cognitive control across tasks	10
Standard GLM analysis of fMRI during emotional movies.....	11
Supplementary tables	12
Supplementary figures	28
Supplementary references	34

Supplementary methods

Experimental data

Part of this dataset was reported in previous work where we focused on changes in resting state brain networks induced by negative emotions (REST1 and REST2 conditions from the two affective contexts¹), and examined how emotional effects on resting state relate to activations evoked by the preceding movie (MOVIE1 and REST1 conditions from the two affective contexts²). These studies used seed-based connectivity analyses based on precuneus and insula activations. The present study concerns only the task-related effects and deploys a fully data-driven seed-free methodology.

Affective stimuli

Previously validated videoclips with strong emotional content were used for emotional induction. Movies were edited from the films “21 Grams”³ and “Sophie's Choice”⁴, both used by previous studies and well characterized in terms of valence, arousal, and type of emotions (i.e. sadness)⁵⁻⁹. Both excerpts included young mothers as main characters, experiencing the loss of their underage children. Participants were instructed to feel as involved as possible in the drama of the movies. We reinforced a first-person perspective by recruiting only female participants, and instructed them to feel involved while watching the movie clip. In addition, neutral clips of 5-minutes were presented in the control conditions, taken from TV documentaries available on the internet, with verbally interacting people generally similar to the sad movie but without any strong emotional aspect. The free software iMovie (<https://www.apple.com/lae/imovie/>) was used for editing. We further validated these stimuli in a preliminary pilot study, where a different group of healthy volunteers (n=28) rated the pleasantness, intensity, and type of emotions elicited by each movie. The final clips were also compared in terms of low-level features (sound level, luminance, spatial frequency and motion), and no significant differences between both conditions were found.

Subjective emotional measurements

Mood questionnaires assessing the participant's affective state were given before and after each experimental context, including the Positive and Negative Affect Scales, PANAS¹⁰. Additionally, participants rated their affective response to each movie with a 9-point Likert scale combined with the self-assessment Manikin, SAM¹¹, as used in previous work^{7,9}. These ratings included valence ("How happy/pleased or unhappy/dissatisfied are you?", 1 = very unhappy, 9 = very happy), arousal ("How awake/aroused or calm/drowsy do you feel?", 1 = very calm, 9 = very aroused), and subjective hedonic experience ("How pleasant or unpleasant was your own experience of the scene?", 1 = very unpleasant, 9 = very pleasant).

Cognitive control task

To test for the effects of negative emotion on cognitive task performance, we used two classic interference paradigms (face Stroop task and number Flanker task), adjusted for fMRI compatibility. Each task comprised 80 trials (40 congruent and 40 incongruent). Individual stimulus presentation lasted 1s, followed by an inter-trial interval with a central fixation cross randomly jittering from 2 to 4.9s. Both tasks were counterbalanced across affective context conditions and across participants. Each task combined congruent (C) and incongruent (I) trials in which a central target (name in Stroop, number in Flanker) was presented for a binary classification response (male/female for Stroop, odd/even for Flanker), together with a distractor corresponding to either the same (C) or opposite (I) response. In addition, a given trial could be preceded by either the same or the opposite condition (C or I trials), in a semi-random but balanced order. This resulted in 4 trial types, allowing subsequent behavioral analysis according to both current compatibility (indicated by upper-case letters "C" and "I") and compatibility of the preceding trial (indicated by lower-case letters "c" and "i", see **Figure S1B** for a schematic description).

Face-name Stroop task

All face images in the Stroop task were obtained from the Karolinska Directed Emotional Faces, KDEF¹². Participants were shown pictures of faces superimposed with names. The name and face corresponded to the same gender in 50% of the trials (congruent stimuli). We used images of 35 male and 35 female faces (portrait format, size 6. cm x 8.5 cm). To obtain some homogeneity of visual features, all images were standardized in terms of color background (grey), color portray (black & white), and face proportion in image (close-up). We used 70 different names from the French language, whose gender association was verified during preliminary piloting. All stimuli were presented on a screen outside the scanner bore, reflected on a mirror placed on the head coil. Participants gave responses with an MRI-compatible device with two key buttons at the right side. The instruction was to categorize the name as male or female. Stimulus size and screen-participant distance were reduced in a 1:2 ratio (approx.) for tasks inside the scanner.

Number Flanker task

The stimuli were digits (1 to 9) presented on a gray background. They were presented with the same font size and color as names in the Stroop task. To control for negative priming, a digit could be repeated as a flanker not less than nine trials after being presented as target. The target digit appeared in the center of the screen, reflected on the head-coil mirror. Two flanker digits were presented to the left and right of the target, 10 mm away from the target. The left and right flanker digits were always the same. The subjects' task was to categorize the central digit as odd or even, and to respond by pressing a left or right response key from the MRI-compatible device. Stimulus size and screen-participant distance were reduced in a 1:2 ratio (approx.) for tasks given inside the scanner.

FMRI data acquisition

Neuroimaging data were collected using a 3T Magnetom TIM Trio scanner (Siemens, Germany) and a 32 channels head-coil. The Blood Oxygenation Level Dependent (BOLD) contrast was measured using a T2*-weighted echo-planar sequence (EPI). 928 functional volumes of 60 axial slices each (TR/TE/flip angle = 1300ms/25ms/60°, FOV=212 mm, resolution=106×106, isotropic voxels of 2 mm³, distance factor 10%) were acquired. Furthermore, we collected a high-resolution T1-weighted anatomical image [TR/TI/TE/flip angle=1900ms/900ms/2.27ms/9°, FOV=256mm, resolution=256×256, slice thickness=1mm³, 192 sagittal slices, phase encoding direction= Anterior-Posterior (AP). Our multiband sequence included 4 dummy scans (~ 5s) at the beginning of the fMRI scanning.

GLM-based fMRI analysis

As a preliminary analysis of the neural correlates of cognitive control, we implemented a GLM analysis in SPM12¹³ including eight covariates of interest representing the stimulus congruency condition for each trial (i.e. cC, iC, il and cl) and the affective context (i.e., “negative” and “neutral”). These regressors were convolved with a standard hemodynamic response function (HRF) according to an event-related design, which was then submitted to a univariate regression analysis. Realignment parameters were added to the design matrices of individual models to account for any residual movement confounds. The design matrix also included low-frequency drifts (cutoff frequency at 1/128 Hz). Flexible factorial analyses of variance (ANOVAs) were then performed on the following contrasts of interest: 1) All “I” vs. “C” trials, comparing incongruent vs. congruent trials regardless of preceding trial and affective context, in order to probe for standard attention-dependent activations related to congruency effects (see results in **Table S**). 2) All trials (cC, iC, il, cl)_{negative} vs. all trials (cC, iC, il, cl)_{neutral}, testing for the main effect of prior affective stimulation on event-related responses to all trial

types, regardless of task condition (see results in **Figure S2B**). Brain activation maps were thresholded with $p_{FWE} < .05$, corrected at the whole brain level, and visualized at $p_{unc} < .001$.

Preprocessing for co-activation pattern (CAP) analysis

Following Bolton et al.,¹⁴ standard image preprocessing procedures were applied using the DPABI toolbox¹⁵. Time-series from each voxel in the white matter and cerebrospinal fluid, plus the six affine motion parameters from realignment (also including their respective first-order derivatives), were used as nuisance variables to be regressed out from the data. No global signal regression (GSR) was carried out given the absence of agreement in the field in this regard¹⁶. Although some studies support this approach^{17,18}, others suggest that GSR does not affect the CAP extraction procedure¹⁹ nor measures of anticorrelation among intrinsic functional brain networks²⁰. Furthermore, the data were band-pass filtered between 0.01 and 0.10 Hz. All image volumes with frame-wise displacement above 0.5 mm were discarded, as well as subjects with more than 30% of scrubbed frames²¹.

Bayesian structural equation modelling (BSEM)

BSEM specification

Four BSEMs comprised the main analysis to investigate how brain networks recruited during the cognitive control task were modulated by dFC patterns during the preceding rest and movie periods, in different emotion contexts. The first multivariate model assessed the relationship between CAPs expressed in the “REST1” condition (predictor variables) and the CAPs observed during the “TASK” condition (outcomes) for both affective contexts. The number of occurrences of each brain CAP was treated as a manifest variable. Correlations between the same CAPs across the affective contexts (e.g., DMN_{CAP} “negative REST1” and DMN_{CAP} “neutral REST1”) were modeled as covariates to represent expected residual associations between regions in different contexts. Subsequently, a second model examined the mediation of behavioral task performance as measured by RT on the

regressions of the first model. The mediator variable was a latent construct measured by the RTs in the cognitive control task trials (i.e., “cC, iC, cI, il” trials). Individual RT scores were multiplied by 10 to bring their variance into the same order of magnitude as the CAP occurrence measures. This improves estimation algorithm performance in BSEM in relation to the CAP occurrences. Finally, two other models were computed with the same characteristics as above, assessing the relationship between CAPs during the “MOVIE2” (predictor variables) and CAPs at the “TASK” condition without and with the behavioral mediation effect. A graphical illustration of these models is found in **Figure S4**. Default values for priors and hyperparameters from the blavaan package were used for the Bayesian estimation:

- Intercept manifest variable (MV) $\sim \text{Norm}(0, 10)$
- Intercept latent variable (LV) $\sim \text{Norm}(0, 10)$
- Loading factor $\sim \text{Norm}(0, 10)$
- Regression $\sim \text{Norm}(0, 10)$
- Precision MV $\sim \Gamma(1, .05)$ (SD)
- Precision LV $\sim \Gamma(1, .05)$ (SD)
- Correlation $\sim \text{Beta}(1, 1)$
- Covariance matrix $\sim \text{Wishart}(3, \text{iden})$
- Threshold $\sim \text{Norm}(0, 1.5)$

Due to the novelty of the implemented approach, it was not possible to find any further dataset with similar features in terms of functional neuromarkers and experimental manipulations to provide more informative priors, so we conservatively chose these uninformative priors. All BSEMs were estimated using 4 Markov Monte Carlo chains (MCMC), 1000 burn-in iterations, and 5000 estimation samples.

BSEM model validation tests and invariance

The first step in structural equation modeling of latent constructs is establishing that the observed variables are measuring the same construct across the experimental blocks²². This is accomplished by constructing a measurement model and testing it for invariance across conditions and affective contexts. This proceeds in steps from configural invariance to strong invariance, to strict invariance

(adding the requirement that the magnitude of unexplained variance for each observed variable does not change across conditions and/or contexts). We implemented specific models for measuring the invariance of the behavioral data, namely, the RTs of cC, iC, il, and cl trials of the cognitive control tasks. This model was then successively constrained to test for weak invariance and strict invariance by examining the fit indices and likelihood ratio chi-square difference tests²². (see results in **Table S9**) In line with previous fMRI works^{23,24}, strong variance was expected in the CAPs data, given the variety of the experimental stimuli and the high sensitivity of the neural functional activity.

Model convergence and priors assessment

The models integrity and the impact of prior distributions was examined in five steps. First, we plotted the four Markov chains for each parameter in order to visualize the sampling behavior and mixing of these chains. The traceplots depicted a satisfactory convergence and mixing (see **Figure S5A**). This was further supported by the Gelman-Rubin diagnostic, which yielded potential scale reduction factor values (PSRF) near 1 for all parameters. See full results in **Table S10**. Second, the parameter estimates of the four chains yielded smooth densities with no indication of boundary conditions (see histograms in **Figure S5B**). Third, the serial autocorrelation assessment yielded a low dependency between estimates. This provided further support for optimality (see detailed results in **Figure S6**). Fourth, the effective sample size (ESS) represents the number of independent samples that have the same precision as the total number of samples in the posterior chains. ESS values ensured enough precision in the chains. Lastly, sensitivity analyses on the direct, indirect and total effects showed reliable and robust priors performance since similar results were obtained when different prior parameters were tested.

Supplementary results

Behavioral indices of cognitive control across tasks

Detailed analyses of the reaction time (RT) in the cognitive tasks demonstrated robust and similar effects in both the Flanker and Stroop tasks, confirming the successful validation and standardization of these paradigms obtained in our piloting testing. First, there was no significant differences in the RT of congruent ["C" trials ($t(23) = 1.73$; $p = \text{n.s.}$)] or incongruent trials ["I" ($t(23) = 1.73$; $p = \text{n.s.}$)] when comparing the two tasks. Second, Pearson correlation analyses denoted a significant and similar statistical relationship between both tasks across participants for their average response times (RTs) in both the congruent ($r = .9$; $p < .0001$) and incongruent trials ($r = .8$; $p < .0001$). Third, an omnibus linear mixed model (LMM) ANOVA with the factors "task" (Stroop and Flanker) and "trial type" (cC, iC, il, cl) revealed no main effect of task [$F(1, 126) = 1.52$; $p = \text{n.s.}$], and no significant interaction between the task and trial type ($[F(1, 126) = 0.9$; $p = \text{n.s.}$].

In addition, post-hoc analyses showed no significant differences for any of the different trial types when both tasks were directly compared [cC trials: $\beta = 9.46$; $t(126) = 1.0$; $p = \text{n.s.}$; iC trials: $\beta = 4.23$, $t(126) = 0.4$; $p = \text{n.s.}$; il trials: $\beta = 14.9$, $t(126) = 1.6$; $p = \text{n.s.}$; cl trials: $\beta = 14.3$; $t(126) = 1.5$; $p = \text{n.s.}$]. Finally, the magnitude of the interference cost on RTs (I minus C) did not differ between the two tasks [$F(1, 23) = 1.3$; $p = \text{n.s.}$; see **Figure SC**]. The impact of negative affect on cognitive control is reported in the main text "Results" section, in **Table S**.

Accuracy data showed a pattern similar to RTs. Pearson coefficients of the accuracy index yielded significant correlations between both tasks for each condition [congruent: ($r(23) = 0.82$; $p < .0001$); incongruent ($r(23) = 0.88$; $p < .0001$), indicating a near perfect trend (positive slope) of similar performance in the two tasks. Accuracy data were also submitted to an LMM-based ANOVA in order to cross-validate our standardization of both tasks. This again revealed no significant difference between the tasks [Stroop and Flanker. $F(1, 126) = 2.2$; $p = \text{n.s.}$], and no significant interaction between

task and trial type ($[F(1,126)= 0.4; p= \text{n.s.}]$). Furthermore, post-hoc analyses revealed no significant differences for “cC” trials [$\beta= 12.68$; 95% CI(-0.11_{lower}, 1.09_{upper}); $p_{FDR}= \text{n.s.}$; $d= 0.48$], “iC” trials [$\beta= -14.96$; 95% CI(-1.18_{lower}, 0.03_{upper}); $p_{FDR}= \text{n.s.}$; $d= -0.57$], “il” trials [$\beta= 7.08$; 95% CI (-0.33_{lower}, 0.87_{upper}); $p_{FDR}= \text{n.s.}$; $d= 0.27$], and “cl” trials [$\beta= 0.52$; 95% CI(-0.06_{lower}, 1.15_{upper}); $p_{FDR}= \text{n.s.}$; $d= 0.54$], respectively. Likewise, the interference cost on accuracy (I minus C) did not differ between the two tasks [$F(1, 23)= 1.73$; $p= \text{n.s.}$]. Finally, affective context did not significantly modulate accuracy performance. Detailed results are provided in **Table S1**.

Standard GLM analysis of fMRI during emotional movies

To verify the effectiveness of emotion induction, we examined brain activation during movie watching with a standard GLM-based analysis. As expected, a comparison of the “negative MOVIE2” vs. “neutral MOVIE2” conditions showed higher activation ($p_{FWE} < .05$) in bilateral visual areas, orbital and lateral prefrontal areas, the insula, and the precuneus, consistent with previous fMRI studies of emotional processing. Results are listed in **Table S2**.

Supplementary tables

LMM – ANOVA

Main effects & Interactions	Reaction time	Accuracy	Main effects & Interactions	Reaction time	Accuracy
Task	$F(1, 161)= 1.52$ $p < \text{n.s.}$	$F(1, 154)= 2.2$ $p < \text{n.s.}$	Emotion	$F(1, 161)= 7.77$ $p < .01$	$F(1, 154)= 0.2$ $p < \text{n.s.}$
Previous trial	$F(1,161)= 0.21$ $p < \text{n.s.}$	$F(1,154)= 1.99$ $p < \text{n.s.}$	Previous trial	$F(1, 161)= 0.07$ $p = \text{n.s.}$	$F(1, 154)= 1.93$ $p = \text{n.s.}$
Current trial	$F(1,161)= 202.11$ $p < .0001$	$F(1,154)= 14.90$ $p < .0001$	Current trial	$F(1, 161)= 215$ $p < .0001$	$F(1, 154)= 14.46$ $p < .0001$
Previous trial vs. Current trial	$F(1,161)= 43.96$ $p < .0001$	$F(1,154)= 0.32$ $p < \text{n.s.}$	Previous trial vs. Current trial	$F(1, 161)= 46.1$ $p < .0001$	$F(1, 154)= 0.69$ $p < \text{n.s.}$
Task vs. Previous trial	$F(1, 161)= 1.1$ $p < \text{n.s.}$	$F(1, 154)= 0.43$ $p < \text{n.s.}$	Emotion vs. Previous trial	$F(1, 161)= 0.02$ $p < \text{n.s.}$	$F(1, 154)= 0.21$ $p < \text{n.s.}$
Task vs. Current trial	$F(1, 161)= 2.34$ $p < \text{n.s.}$	$F(1, 154)= 0.43$ $p < \text{n.s.}$	Emotion vs. Current trial	$F(1, 161)= 1.51$ $p < \text{n.s.}$	$F(1, 154)= 0.21$ $p < \text{n.s.}$
Task vs. Previous vs. Current	$F(1, 161)= 1.79$ $p < \text{n.s.}$	$F(1, 154)= 0.43$ $p < \text{n.s.}$	Emotion vs. Previous vs. Current	$F(1, 161)= 6.82$ $p < .01$	$F(1, 154)= 0.01$ $p < \text{n.s.}$

Table S1. Mixed model analysis (LMM) of reaction time and accuracy in the cognitive control tasks. **Left.** LMM results assessing the “task effect” (i.e., Stroop vs. Flanker) on congruency effect (CE) and congruency sequence effect (CSE). **Right.** A second set of LMM assessed the “emotion effect” (i.e., neutral vs. negative) on the congruency effect (CE) and congruency sequence effect (CSE) respectively. Post-hoc contrasts analyses were adjusted for multiple comparisons with the FDR (false discovery rate) method.

Brain Region	Coordinates (MNI)			K	Z-score
	x	y	z		
Congruent > Incongruent					
Hippocampus	-22	-38	-4	119	5.91
Incongruent > Congruent					
Superior parietal lobe	-22	-62	46	784	8.04
Superior parietal lobe	28	-68	30	675	5.39
Middle frontal gyrus	-24	4	48	188	6.33
Supplementary motor C.	-80	20	48	250	5.43
Inferior temporal gyrus	-48	-66	-16	372	5.07
Inferior temporal gyrus	46	-62	-14	129	5.01
Middle occipital gyrus	36	-82	12	287	5.29
Middle frontal gyrus	-40	26	22	140	5.81
Middle frontal gyrus	42	10	34	126	5.08
Putamen	-22	0	4	118	4.73
Putamen	28	8	4	328	5.49

Table S2. Standard GLM analysis of fMRI depicting brain activation during cognitive control tasks. Top part. As expected, few brain regions showed increased activity in the contrast comparing congruent and incongruent trials ($C > I$). The bottom part describe the brain regions with increased activity in the opposite contrast ($I > C$). Cluster defining threshold ($p_{UNC} < .001$), corrected critical cluster size ($p_{FWE} < .05$).

DESCRIPTIVE STATISTICS

CAP	CONDITION	MEAN	SD	MEDIA	MAD	skew	SE	IQR	Q _{0.25}	Q _{0.5}	Q _{0.75}	R _{MIN}	R _{MAX}
DMN	NEUTRAL REST 1	55,5	13,7	56,5	12,6	-0,1	2,8	16,5	46,8	56,5	63,3	25	81
	NEUTRAL MOVIE 2	52,5	8,4	51,0	8,2	-0,3	1,7	9,3	49,0	51,0	58,3	35	66
	NEUTRAL TASK	51,2	8,4	52,0	5,9	-0,8	1,7	8,5	48,0	52,0	56,5	29	63
	AFFECTIVE REST 1	58,5	10,8	57,0	9,6	0,6	2,2	11,3	52,3	57,0	63,5	39	86
	AFFECTIVE MOVIE 2	51,7	5,5	51,5	5,2	-0,2	1,1	6,0	49,0	51,5	55,0	39	65
	AFFECTIVE TASK	55,0	8,2	54,0	5,9	0,8	1,7	8,0	50,0	54,0	58,0	41	78
SN-SMN	NEUTRAL REST 1	50,6	10,7	48,5	5,2	0,6	2,2	10,0	45,0	48,5	55,0	26	81
	NEUTRAL MOVIE 2	51,9	7,0	52,0	6,7	0,9	1,4	8,0	47,0	52,0	55,0	42	73
	NEUTRAL TASK	50,5	8,2	49,5	6,7	0,6	1,7	9,5	46,8	49,5	56,3	35	73
	AFFECTIVE REST 1	51,8	6,5	51,0	5,9	0,3	1,3	7,0	48,5	51,0	55,5	41	68
	AFFECTIVE MOVIE 2	54,6	7,9	52,0	5,9	0,9	1,6	10,3	49,0	52,0	59,3	43	77
	AFFECTIVE TASK	59,0	6,4	59,0	5,2	0,1	1,3	7,3	54,8	59,0	62,0	46	73
VIS	NEUTRAL REST 1	41,0	10,5	42,5	10,4	0,0	2,1	15,0	32,5	42,5	47,5	21	64
	NEUTRAL MOVIE 2	43,2	6,2	43,0	7,4	0,1	1,3	10,3	38,0	43,0	48,3	33	56
	NEUTRAL TASK	44,6	6,9	43,5	6,7	0,5	1,4	7,5	40,5	43,5	48,0	33	62
	AFFECTIVE REST 1	52,2	8,4	51,5	8,2	-0,3	1,7	11,0	47,5	51,5	58,5	35	65
	AFFECTIVE MOVIE 2	55,5	5,9	55,5	5,9	-0,3	1,2	7,5	52,8	55,5	60,3	43	65
	AFFECTIVE TASK	49,0	7,8	48,0	10,4	0,4	1,6	10,5	44,8	48,0	55,3	37	66
FPN	NEUTRAL REST 1	35,7	7,9	36,0	8,2	0,1	1,6	11,3	29,8	36,0	41,0	20	53
	NEUTRAL MOVIE 2	37,8	5,6	38,0	4,4	-0,1	1,1	6,3	35,0	38,0	41,3	27	48
	NEUTRAL TASK	43,9	3,3	43,5	3,7	0,2	0,7	4,3	41,8	43,5	46,0	39	51
	AFFECTIVE REST 1	49,6	7,2	50,0	8,2	-0,2	1,5	9,8	44,8	50,0	54,5	35	61
	AFFECTIVE MOVIE 2	47,5	6,7	47,5	6,7	-0,1	1,4	8,3	43,8	47,5	52,0	31	63
	AFFECTIVE TASK	54,9	5,4	54,0	5,9	-0,1	1,1	8,5	50,8	54,0	59,3	43	63

Table S3. Summary statistics of temporal occurrences for all CAPs for each CAP and each experimental condition. SD: Standard deviation. MAD: Median absolute deviation. SE: Standard error. IQR: Interquartile range. R_{MIN}: Low range. R_{MIN}: High range

LMMs FACTORIAL ANOVA

CAP	CONTEXT NEU. – NEG.	CONDITION REST1 - MOVIE2 - TASK	INTERACTION CONDITION X CONTEXT	CONTRASTS EMMEANS	CI LOW	CI HIGH	p FDR	d COHEN
DMN	$F(1,115) = 1.84$ $p = \text{n.s.}$ $\eta^2 = .02$ <i>CI</i> 95% (0.00, 1.00)	$F(2,115) = 4.25$ $p < .05$ $\eta^2 = .07$ <i>CI</i> 95% (0.01, 1.00)	$F(2,115) = 0.40$ $p = \text{n.s.}$ $\eta^2 = .02$ <i>CI</i> 95% (0.00, 1.00)	NEU MOVIE2 - NEU REST1	-0.92	0.22	.30	.34
				NEU MOVIE2 - NEU TASK	-0.42	0.78	.88	.14
				NEU REST1 - NEU TASK	-0.07	1.06	.37	.49
				NEG MOVIE2 - NEG REST1	-1.35	-0.20	.02	.77
				NEG MOVIE2 - NEG TASK	-0.94	0.20	.24	.37
				NEG REST1 - NEG TASK	-0.16	0.98	.51	.40
				NEG REST1 - NEU REST1	-0.23	0.91	.53	.34
				NEU MOVIE2 - NEU REST1	-0.39	0.75	.88	.18
SN-SMN	$F(1,115) = 12.31$ $p < .001$ $\eta^2 = .10$ <i>CI</i> 95% (0.03, 1.00)	$F(2,115) = 2.21$ $p = \text{n.s.}$ $\eta^2 = .04$ <i>CI</i> 95% (0.00, 1.00)	$F(2,115) = 4.53$ $p = \text{n.s.}$ $\eta^2 = .02$ <i>CI</i> 95% (0.00, 1.00)	NEU MOVIE2 - NEU TASK	-0.37	0.77	.88	.20
				NEU REST1 - NEU TASK	-0.55	0.58	.66	.02
				NEG MOVIE2 - NEG REST1	-0.96	0.17	.07	.39
				NEG MOVIE2 - NEG TASK	-1.61	-0.44	<.0001	1.02
				NEG REST1 - NEG TASK	-1.21	-0.05	.01	.63
				NEG TASK - NEU TASK	0.62	1.80	.001	1.21
				NEU MOVIE2 - NEU REST1	-0.25	0.89	.28	.32
				NEU MOVIE2 - NEU TASK	-0.79	0.35	.44	.22
VIS	$F(1,115) = 70.67$ $p < .001$ $\eta^2 = .38$ <i>CI</i> 95% (0.03, 1.00)	$F(2,115) = 2.48$ $p = .09$ $\eta^2 = .04$ <i>CI</i> 95% (0.00, 1.00)	$F(2,115) = 5.09$ $p < .01$ $\eta^2 = .08$ <i>CI</i> 95% (0.01, 1.00)	NEU REST1 - NEU TASK	-1.18	0.03	.08	.54
				NEG MOVIE2 - NEG REST1	-0.08	1.06	.11	.49
				NEG MOVIE2 - NEG TASK	0.39	1.56	.0002	.98
				NEG REST1 - NEG TASK	-0.08	1.06	0.11	.49
				NEG MOVIE2 - NEU MOVIE2	1.24	2.47	<.0001	1.89
				NEU MOVIE2 - NEU REST1	-0.23	0.91	0.11	.34
				NEU MOVIE2 - NEU TASK	-1.56	-0.39	<.0001	.97
				NEU REST1 - NEU TASK	-1.91	-0.72	<.0001	1.32
FPN	$F(1,138) = 123.63$ $p < .0001$ $\eta^2 = .47$ <i>CI</i> 95% (0.47, 1.00)	$F(2,138) = 18.84$ $p < .0001$ $\eta^2 = .21$ <i>CI</i> 95% (0.12, 1.00)	$F(2,138) = 1.41$ $p = \text{n.s.}$ $\eta^2 = .02$ <i>CI</i> 95% (0.00, 1.00)	NEG MOVIE2 - NEG REST1	-0.90	0.24	.0002	.33
				NEG MOVIE2 - NEG TASK	-1.77	-0.59	<.0001	1.18
				NEG REST1 - NEG TASK	-1.43	-0.28	<.0001	.86
				NEG TASK - NEU TASK	1.15	2.37	<.0001	2.37

Table S4. LMM analyses of the temporal occurrences of CAPs across conditions were computed using a 2x3 factorial design the factors “context” (neutral vs. negative), “condition” (“REST1”, “MOVIE2”, and “TASK”). The percent of partial variance explained η^2 expresses the effect size of the main effects and interactions. Post-hoc pairwise least squared means contrasts (EMMEANS) driving the main effects and interactions are listed in the right-hand columns. Significance indices (p_{FDR}) are adjusted for multiple testing under dependency. Effects size (d_{Cohen}) are reported in absolute values.

MEASUREMENT INVARIANCE								
CONDITION	INVARIANCE	df	AIC	BIC	χ^2	Δdf	$\Delta \chi^2$	P
TASK (REACTION TIME)	Baseline	19	1902	1932	21	3	4.5	.22
	Configural	22	1901	1927	26			
	Configural	22	1901	1927	25	4	16.3	.003
	Strong	26	1909	1930	42			
	Strong	26	1909	1930	45	3	9,9	.02
	Strict	29	1913	1931	52			

Table S5. Results of the measurement model fitting and invariance testing. *Df*: Degrees of freedom, AIC: Akaike information criterion. BIC: Bayesian information criterion. χ^2 : Chi-squared. Δdf : change in degrees of freedom. $\Delta \chi^2$: Chi-squared difference between two invariance models (e.g., Baseline vs. Configural). *P*: The χ^2 *p*-value.

POTENTIAL SCALE REDUCTION FACTOR VALUES (PSRF)

	PARAMETERS AIM1	\hat{R}	PARAMETERS AIM2	\hat{R}
NEUTRAL	RT ~ DMN	1.0002	RT ~ DMN	1.0001
	RT ~ SN-SMN	1.0000	RT ~ SN-SMN	1.0000
	RT ~ VIS	1.0001	RT ~ VIS	1.0002
	RT ~ FPN	1.0001	RT ~ FPN	0.9999
	DMN ~ DMN	1.0000	DMN ~ DMN	0.9999
	DMN ~ SN-SMN	1.0000	DMN ~ SN-SMN	0.9999
	DMN ~ VIS	0.9999	DMN ~ VIS	0.9999
	DMN ~ FPN	1.0000	DMN ~ FPN	1.0000
	SN-SMN ~ DMN	1.0003	SN-SMN ~ DMN	1.0001
	SN-SMN ~ SMN	1.0003	SN-SMN ~ SMN	1.0000
	SN-SMN ~ VIS	0.9999	SN-SMN ~ VIS	0.9999
	SN-SMN ~ FPN	1.0000	SN-SMN ~ FPN	1.0001
	VIS ~ DMN	1.0000	VIS ~ DMN	1.0000
	VIS ~ SMN	1.0001	VIS ~ SMN	1.0000
	VIS ~ VIS	1.0000	VIS ~ VIS	1.0000
	VIS ~ FPN	0.9999	VIS ~ FPN	0.9999
	FPN ~ DMN	0.9999	FPN ~ DMN	0.9999
	FPN ~ SN-SMN	0.9999	FPN ~ SN-SMN	1.0000
	FPN ~ VIS	0.9999	FPN ~ VIS	1.0000
	FPN ~ FPN	1.0000	FPN ~ FPN	1.0000
NEGATIVE	RT ~ DMN	1.0001	RT ~ DMN	1.0002
	RT ~ SN-SMN	0.9999	RT ~ SN-SMN	1.0001
	RT ~ VIS	1.0003	RT ~ VIS	0.9999
	RT ~ FPN	1.0000	RT ~ FPN	1.0001
	DMN ~ DMN	0.9999	DMN ~ DMN	0.9999
	DMN ~ SN-SMN	0.9998	DMN ~ SN-SMN	1.0002
	DMN ~ VIS	0.9999	DMN ~ VIS	0.9999
	DMN ~ FPN	0.9999	DMN ~ FPN	1.0000
	SN-SMN ~ DMN	1.0000	SN-SMN ~ DMN	0.9999
	SN-SMN ~ SMN	0.9999	SN-SMN ~ SMN	1.0000
	SN-SMN ~ VIS	0.9999	SN-SMN ~ VIS	1.0002
	SN-SMN ~ FPN	1.0000	SN-SMN ~ FPN	1.0001
	VIS ~ DMN	0.9999	VIS ~ DMN	0.9999
	VIS ~ SMN	0.9998	VIS ~ SMN	1.0000
	VIS ~ VIS	1.0001	VIS ~ VIS	1.0000
	VIS ~ FPN	0.9999	VIS ~ FPN	1.0000
	FPN ~ DMN	1.0000	FPN ~ DMN	1.0000
	FPN ~ SN-SMN	1.0001	FPN ~ SN-SMN	1.0000
	FPN ~ VIS	0.9999	FPN ~ VIS	1.0003
	FPN ~ FPN	1.0000	FPN ~ FPN	1.0000

Table S6. Results of the Gelman and Rubin diagnostic for the BSEM. The potential scale reduction factors (\hat{R}) near one provides an estimation of convergence for each regression (parameter) in the models assessing hypothesis 1 (left) and hypothesis 2 (right).

EFFECTIVE EFFECT SIZE (EES)				
	AIM1		AIM2	
	PARAMETER	EES	PARAMETER	EES
NEUTRAL	RT ~ DMN	4973,9	RT ~ DMN	15886,0
	RT ~ SN-SMN	3787,5	RT ~ SN-SMN	14755,5
	RT ~ VIS	4386,7	RT ~ VIS	12276,6
	RT ~ FPN	5154,5	RT ~ FPN	14919,3
	DMN ~ DMN	4073,4	DMN ~ DMN	23131,2
	DMN ~ SN-SMN	3517,8	DMN ~ SN-SMN	23865,6
	DMN ~ VIS	3975,0	DMN ~ VIS	25357,6
	DMN ~ FPN	4684,0	DMN ~ FPN	21573,5
	SN-SMN ~ DMN	3822,1	SN-SMN ~ DMN	22384,5
	SN-SMN ~ SMN	3150,2	SN-SMN ~ SMN	22023,9
	SN-SMN ~ VIS	3867,9	SN-SMN ~ VIS	23163,3
	SN-SMN ~ FPN	4188,9	SN-SMN ~ FPN	22594,3
	VIS ~ DMN	4032,5	VIS ~ DMN	23382,0
	VIS ~ SMN	3684,7	VIS ~ SMN	25582,2
	VIS ~ VIS	4119,2	VIS ~ VIS	26426,0
	VIS ~ FPN	4834,6	VIS ~ FPN	21875,7
	FPN ~ DMN	7080,2	FPN ~ DMN	23278,0
	FPN ~ SN-SMN	5849,3	FPN ~ SN-SMN	21446,0
	FPN ~ VIS	6939,8	FPN ~ VIS	18802,3
	FPN ~ FPN	7547,4	FPN ~ FPN	21866,2
NEGATIVE	RT ~ DMN	4788,8	RT ~ DMN	11327,9
	RT ~ SN-SMN	4591,1	RT ~ SN-SMN	11768,7
	RT ~ VIS	4369,8	RT ~ VIS	15207,2
	RT ~ FPN	4762,3	RT ~ FPN	15108,4
	DMN ~ DMN	33,2	DMN ~ DMN	22824,7
	DMN ~ SN-SMN	98,3	DMN ~ SN-SMN	19303,2
	DMN ~ VIS	204,7	DMN ~ VIS	22653,0
	DMN ~ FPN	190,7	DMN ~ FPN	22531
	SN-SMN ~ DMN	25,3	SN-SMN ~ DMN	23559,7
	SN-SMN ~ SMN	65,0	SN-SMN ~ SMN	17123,9
	SN-SMN ~ VIS	142,4	SN-SMN ~ VIS	21952,9
	SN-SMN ~ FPN	145,9	SN-SMN ~ FPN	21368,4
	VIS ~ DMN	24,1	VIS ~ DMN	22453,7
	VIS ~ SMN	69,6	VIS ~ SMN	15347,6
	VIS ~ VIS	165,1	VIS ~ VIS	22797,8
	VIS ~ FPN	167,2	VIS ~ FPN	21770,3
	FPN ~ DMN	686,0	FPN ~ DMN	18414,0
	FPN ~ SN-SMN	3349,1	FPN ~ SN-SMN	17032,7
	FPN ~ VIS	3512,0	FPN ~ VIS	21391,7
	FPN ~ FPN	3318,7	FPN ~ FPN	19726,0

Table S7. Results of the effective effect size (EES) for the BSEM. EES values >1 confirmed an optimal stability in the parameter estimation of the models related to hypothesis 1 (left) and hypothesis 2 (right).

SENSITIVITY ANALYSES					
Parameter	Parameter	Estimate with N(0,10)	Bias (%) with N(-10,0)	Bias (%) with N(-5,5)	Bias (%) with N(0,100)
AIM 1	DMN ~ RT	0,38	-15,80	2,20	0,92
	RT ~ FPN	0,31	-6,74	3,28	12,28
	DMN ~ FPN	0,43	-14,77	2,34	-5,98
	SN SMN ~ RT	-0,31	19,17	5,16	5,16
	SN SMN ~ FPN	-0,39	-3,42	-1,44	-1,06
AIM 2	SN SMN ~ RT	0,46	-27,91	2,22	-2,51
	RT ~ FPN	0,36	-62,24	-1,28	-2,80
	SN SMN ~ FPN	0,49	-68,66	2,70	16,61

Table S8. Results of the sensitivity analysis. Results from different prior distributions yielded small percentage deviation (i.e., <50% bias) when different prior scenarios (e.g., N (-5,5); N (0,100)) were examined in relation to our diffuse prior distribution (i.e., N (0,10)). Small bias indicate low influence of both informative and more diffuse priors on the obtained results. As expected, improper prior distributions (e.g., N(-10, 0) in which all the beta regressions have negative values) yielded inadmissible solutions (i.e., >50% bias) in some of the estimations. Together, the sensitivity analysis confirmed a low impact of the priors on the results.

DIRECT EFFECTS AIM1

	CAPS REST1 (X)	CAPS TASK (Y)	MEDIAN	CI (LOW)	CI (HIGH)	PD (%)	IN ROPE (%)
NEUTRAL CONTEXT	DMN _{REST1}	RT _{TASK}	0.18	-0.11	0.36	83	10
	SN-SMN _{REST1}	RT _{TASK}	-0.08	-0.21	0.45	66	50
	VIS _{REST1}	RT _{TASK}	0.19	-0.13	0.28	88	13
	FPN _{REST1}	RT _{TASK}	0.21	-0.19	0.43	09	22
	RT _{TASK}	DMN _{TASK}	-0.2	-0.7	0.27	81	25
	RT _{TASK}	SN-SMN _{TASK}	0.33	-0.17	0.84	91	14
	RT _{TASK}	VIS _{TASK}	0.1	-0.42	0.57	66	32
	RT _{TASK}	FPN _{TASK}	0.35	0.16	0.55	100	00
	DMN _{REST1}	DMN _{TASK}	0.39	0.04	0.86	98	03
	SN-SMN _{REST1}	DMN _{TASK}	0.01	-0.52	0.52	51	31
	VIS _{REST1}	DMN _{TASK}	0.27	-0.06	0.62	94	14
	FPN _{REST1}	DMN _{TASK}	0.21	-0.14	0.38	919	20
	DMN _{REST1}	SN-SMN _{TASK}	0.22	-0.26	0.71	82	23
	SN-SMN _{REST1}	SN-SMN _{TASK}	0.2	-0.32	0.75	78	24
	VIS _{REST1}	SN-SMN _{TASK}	0.21	-0.16	0.58	86	21
	FPN _{REST1}	SN-SMN _{TASK}	0.17	-0.26	0.59	79	29
	DMN _{REST1}	VIS _{TASK}	-0.08	-0.53	0.38	63	34
	SN-SMN _{REST1}	VIS _{TASK}	0.38	-0.13	0.87	93	11
	VIS _{REST1}	VIS _{TASK}	0.25	-0.1	0.59	93	17
	FPN _{REST1}	VIS _{TASK}	0.26	-0.13	0.68	90	18
	DMN _{REST1}	FPN _{TASK}	0.59	0.14	1.06	100	00
	SN-SMN _{REST1}	FPN _{TASK}	-0.12	-0.31	0.19	87	41
	VIS _{REST1}	FPN _{TASK}	0.11	-0.04	0.26	93	46
	FPN _{REST1}	FPN _{TASK}	0.11	-0.07	0.28	89	48

Table S9. Supplementary results from the Bayesian structural equation modelling (BSEM). Direct effects of the relationship between brain CAPs in the “REST1” condition and brain CAPs in the “TASK” condition, neutral context. Median: standardized coefficients of the predictive role for each direct effect. CI_{LOW} - CI_{HIGH}: Range of the ROPE confidence interval (CI/ 95%). PD: (Probability of Direction) index of effect existence. Significance criterion for the posterior distribution values: <2,5% in ROPE.

DIRECT EFFECTS AIM1

	CAPS REST1 (X)	CAPS TASK (Y)	MEDIAN	CI (LOW)	CI (HIGH)	PD (%)	IN ROPE (%)
NEGATIVE CONTEXT	DMN _{REST1}	RT _{TASK}	0.46	0.17	0.81	99	01
	SN-SMN _{REST1}	RT _{TASK}	-0.48	-0.88	-0.08	99	02
	VIS _{REST1}	RT _{TASK}	0.18	-0.05	0.42	94	25
	FPN _{REST1}	RT _{TASK}	-0.01	-0.29	0.26	54	57
	RT _{TASK}	DMN _{TASK}	-0.19	-0.87	0.52	72	21
	RT _{TASK}	SN-SMN _{TASK}	0.13	-0.4	0.68	69	27
	RT _{TASK}	VIS _{TASK}	0.35	-0.36	1.03	85	14
	RT _{TASK}	FPN _{TASK}	0.69	0.26	1.16	100	00
	DMN _{REST1}	DMN _{TASK}	0.45	0.02	0.86	98	02
	SN-SMN _{REST1}	DMN _{TASK}	0.18	-0.25	0.59	82	27
	VIS _{REST1}	DMN _{TASK}	0.04	-0.32	0.39	59	45
	FPN _{REST1}	DMN _{TASK}	0.25	-0.1	0.49	92	19
	DMN _{REST1}	SN-SMN _{TASK}	0.04	-0.3	0.35	06	48
	SN-SMN _{REST1}	SN-SMN _{TASK}	0.08	-0.24	0.41	07	43
	VIS _{REST1}	SN-SMN _{TASK}	0.02	-0.25	0.3	57	56
	FPN _{REST1}	SN-SMN _{TASK}	-0.75	-1.41	-0.10	100	00
	DMN _{REST1}	VIS _{TASK}	-0.09	-0.51	0.32	68	36
	SN-SMN _{REST1}	VIS _{TASK}	0.26	-0.16	0.69	89	18
	VIS _{REST1}	VIS _{TASK}	0.45	0.1	0.81	99	00
	FPN _{REST1}	VIS _{TASK}	-0.01	-0.43	0.44	51	38
	DMN _{REST1}	FPN _{TASK}	0.43	0.20	0.68	53	00
	SN-SMN _{REST1}	FPN _{TASK}	-0.39	-0.49	-0.09	99	02
	VIS _{REST1}	FPN _{TASK}	0.10	-0.15	0.35	80	46
	FPN _{REST1}	FPN _{TASK}	0.04	-0.25	0.34	60	52

Table S10. Supplementary results from the Bayesian structural equation modelling (BSEM). Direct effects of the relationship between brain CAPs in the “REST1” condition and brain CAPs in the “TASK” condition, negative context. Median: standardized coefficients of the predictive role for each direct effect. CI_{LOW}-CI_{HIGH}: Range of the ROPE confidence interval (CI 95%). PD: (Probability of Direction) index of effect existence. Significance criterion for the posterior distribution values: <2,5% in ROPE.

INDIRECT EFFECTS AIM1

	CAPS REST1 (X)	REACTION TIME (M)	CAPS TASK (Y)	MEDIAN	CI (LOW)	CI (HIGH)	PD (%)	IN ROPE (%)
NEUTRAL CONTEXT	DMN	RT	DMN	-0.04	-0.27	0.11	08	71
	SN-SMN	RT	DMN	0.02	-0.16	0.17	06	94
	VIS	RT	DMN	-0.05	-0.24	0.09	08	75
	FPN	RT	DMN	-0.04	-0.19	0.29	76	86
	DMN	RT	SN-SMN	0.06	-0.07	0.33	89	54
	SN-SMN	RT	SN-SMN	-0.03	-0.15	0.2	63	86
	VIS	RT	SN-SMN	0.06	-0.06	0.3	09	58
	FPN	RT	SN-SMN	0.07	-0.06	0.25	84	73
	DMN	RT	VIS	0.02	-0.14	0.24	65	80
	SN-SMN	RT	VIS	-0.01	-0.1	0.13	56	97
	VIS	RT	VIS	0.02	-0.12	0.21	65	84
	FPN	RT	VIS	0.02	-0.11	0.17	64	92
	DMN	RT	FPN	0.06	-0.13	0.25	98	47
	SN-SMN	RT	FPN	-0.03	-0.11	0.17	66	88
	VIS	RT	FPN	0.07	-0.10	0.22	99	53
	FPN	RT	FPN	0.07	-0.03	0.2	92	72
NEGATIVE CONTEXT	DMN	RT	DMN	-0.07	-0.29	0.15	72	69
	SN-SMN	RT	DMN	0.06	-0.31	0.17	72	65
	VIS	RT	DMN	-0.03	-0.2	0.11	69	87
	FPN	RT	DMN	0.0	-0.12	0.12	52	97
	DMN	RT	SN-SMN	0.05	-0.12	0.22	69	80
	SN-SMN	RT	SN-SMN	-0.04	-0.13	0.25	69	76
	VIS	RT	SN-SMN	0.02	-0.08	0.16	68	92
	FPN	RT	SN-SMN	0.00	-0.09	0.09	43	18
	DMN	RT	VIS	0.13	-0.1	0.35	85	55
	SN-SMN	RT	VIS	-0.11	-0.22	0.36	85	52
	VIS	RT	VIS	0.06	-0.07	0.24	81	76
	FPN	RT	VIS	0.0	-0.15	0.15	52	22
	DMN	RT	FPN	0.32	0.10	0.61	99	02
	SN-SMN	RT	FPN	-0.33	-0.61	-0.09	99	01
	VIS	RT	FPN	0.12	-0.04	0.31	94	44
	FPN	RT	FPN	0.03	-0.22	0.19	54	75

Table S11. Supplementary results from the Bayesian structural equation modelling (BSEM) mediation analyses. Indirect effects of the relationship between brain CAPs of the “REST1” condition and brain CAPs of the “TASK” condition, mediated by the reaction time of the cognitive control tasks. Median: standardized coefficients of the predictive role for each direct effect. $CI_{LOW} - CI_{HIGH}$: Range of the ROPE confidence interval (CI 95%). PD: (Probability of Direction) index of effect existence. Significance criterion for the posterior distribution values: <2,5% in ROPE.

TOTAL EFFECTS AIM1								
	CAPS REST1 (X)	REACTION TIME (M)	CAPS TASK (Y)	MEDIAN	CI (LOW)	CI (HIGH)	PD (%)	IN ROPE (%)
NEUTRAL CONTEXT	DMN	RT	DMN	0.35	0.1	0.85	99	00
	SN-SMN	RT	DMN	0.03	-0.57	0.51	51	31
	VIS	RT	DMN	0.23	-0.11	0.53	61	23
	FPN	RT	DMN	0.17	-0.04	0.66	76	75
	DMN	RT	SN-SMN	0.28	-0.14	0.77	73	43
	SN-SMN	RT	SN-SMN	0.17	-0.32	0.78	79	22
	VIS	RT	SN-SMN	0.27	-0.04	0.66	96	10
	FPN	RT	SN-SMN	0.24	-0.18	0.68	86	21
	DMN	RT	VIS	-0.06	-0.46	0.37	58	37
	SN-SMN	RT	VIS	0.37	-0.15	0.87	93	11
	VIS	RT	VIS	0.27	-0.03	0.61	96	10
	FPN	RT	VIS	0.28	-0.13	0.68	92	15
	DMN	RT	FPN	0.65	0.14	0.92	100	00
	SN-SMN	RT	FPN	-0.15	-0.33	0.16	79	48
	VIS	RT	FPN	0.18	-0.06	0.39	95	73
	FPN	RT	FPN	0.18	-0.02	0.38	97	20
NEGATIVE CONTEXT	DMN	RT	DMN	0.38	0.08	0.71	99	01
	SN-SMN	RT	DMN	0.24	-0.26	0.53	74	34
	VIS	RT	DMN	0.01	-0.35	0.36	52	45
	FPN	RT	DMN	0.25	-0.09	0.35	89	22
	DMN	RT	SN-SMN	0.09	-0.16	0.32	74	53
	SN-SMN	RT	SN-SMN	0.04	-0.18	0.45	8	38
	VIS	RT	SN-SMN	0.04	-0.22	0.35	64	53
	FPN	RT	SN-SMN	-0.75	-1.4	-0.14	100	00
	DMN	RT	VIS	0.04	-0.3	0.32	53	51
	SN-SMN	RT	VIS	0.15	-0.01	0.78	97	06
	VIS	RT	VIS	0.51	0.16	0.88	100	00
	FPN	RT	VIS	-0.01	-0.43	0.43	52	38
	DMN	RT	FPN	0.75	0.02	0.44	100	00
	SN-SMN	RT	FPN	-0.72	-1.3	-0.08	100	00
	VIS	RT	FPN	0.22	-0.05	0.48	95	16
	FPN	RT	FPN	0.03	-0.28	0.34	57	50

Table S12. Supplementary results from the Bayesian structural equation modelling (BSEM) mediation analyses. Total effects of the relationship between brain CAPs in the “REST1” condition and brain CAPs in the “TASK” condition, mediated by the mean reaction time in the cognitive control tasks. Median: standardized coefficients of the predictive role for each direct effect. $CI_{LOW} - CI_{HIGH}$: Range of the ROPE confidence interval (CI 95%). PD: (Probability of Direction) index of effect existence, representing the certainty associated with the most probable direction of the effect. Statistical significance of the posterior distribution values was based on the HDI+ROPE decision rule²⁵ (<2,5% in ROPE).

DIRECT EFFECTS AIM2

	CAPS MOVIE2 (X)	CAPS TASK (Y)	MEDIAN	CI (LOW)	CI (HIGH)	PD (%)	IN ROPE (%)
NEUTRAL CONTEXT	DMN _{MOVIE2}	RT _{TASK}	0.25	-0.05	0.48	99	15
	SN-SMN _{MOVIE2}	RT _{TASK}	0.21	-0.04	0.58	99	14
	VIS _{MOVIE2}	RT _{TASK}	0.23	-0.07	0.55	94	18
	FPN _{MOVIE2}	RT _{TASK}	0.23	-0.08	0.58	93	20
	RT _{TASK}	DMN _{TASK}	-0.04	-0.67	0.57	56	27
	RT _{TASK}	SN-SMN _{TASK}	0.18	-0.19	0.46	85	17
	RT _{TASK}	VIS _{TASK}	0.10	-0.63	0.35	72	29
	RT _{TASK}	FPN _{TASK}	0.30	0.13	0.69	100	00
	DMN _{MOVIE2}	DMN _{TASK}	0.22	-0.02	0.87	97	16
	SN-SMN _{MOVIE2}	DMN _{TASK}	0.08	-0.35	0.43	63	35
	VIS _{MOVIE2}	DMN _{TASK}	0.25	-0.44	0.64	85	20
	FPN _{MOVIE2}	DMN _{TASK}	0.32	0.05	1.01	99	06
	DMN _{MOVIE2}	SN-SMN _{TASK}	0.25	-0.14	0.64	89	40
	SN-SMN _{MOVIE2}	SN-SMN _{TASK}	0.15	-0.25	0.56	77	31
	VIS _{MOVIE2}	SN-SMN _{TASK}	0.24	-0.19	0.7	86	21
	FPN _{MOVIE2}	SN-SMN _{TASK}	-0.16	-0.77	0.44	70	24
	DMN _{MOVIE2}	VIS _{TASK}	0.17	-0.18	0.52	84	29
	SN-SMN _{MOVIE2}	VIS _{TASK}	0.13	-0.22	0.48	78	35
	VIS _{MOVIE2}	VIS _{TASK}	0.18	-0.3	0.35	97	16
	FPN _{MOVIE2}	VIS _{TASK}	0.24	-0.07	0.98	95	07
	DMN _{MOVIE2}	FPN _{TASK}	0.08	-0.05	0.2	89	66
	SN-SMN _{MOVIE2}	FPN _{TASK}	-0.02	-0.16	0.12	61	87
	VIS _{MOVIE2}	FPN _{TASK}	0.09	-0.08	0.26	85	56
	FPN _{MOVIE2}	FPN _{TASK}	0.42	0.1	0.87	100	01

Table S13. Supplementary results from the Bayesian structural equation modelling (BSEM). Direct effects of the relationship between brain CAPs in the “MOVIE2” condition and brain CAPs in the “TASK” condition, neutral context. Median: standardized coefficients of the predictive role for each direct effect. CI_{LOW}-CI_{HIGH}: Range of the ROPE confidence interval (CI 95%). PD: (Probability of Direction) index of effect existence. Significance criterion for the posterior distribution values: <2,5% in ROPE.

DIRECT EFFECTS AIM2

	CAPS MOVIE2 (X)	CAPS TASK (Y)	MEDIAN	CI (LOW)	CI (HIGH)	PD (%)	IN ROPE (%)
NEGATIVE CONTEXT	DMN _{MOVIE2}	RT _{TASK}	0.08	-0.17	0.34	73	52
	SN-SMN _{MOVIE2}	RT _{TASK}	0.46	0.2	0.75	100	00
	VIS _{MOVIE2}	RT _{TASK}	0.15	-0.1	0.41	89	34
	FPN _{MOVIE2}	RT _{TASK}	0.16	-0.06	0.42	92	28
	RT _{TASK}	DMN _{TASK}	0.09	-0.65	0.86	60	22
	RT _{TASK}	SN-SMN _{TASK}	-0.22	-0.78	0.3	81	22
	RT _{TASK}	VIS _{TASK}	0.37	-0.37	1.12	84	13
	RT _{TASK}	FPN _{TASK}	0.59	0.2	0.81	100	00
	DMN _{MOVIE2}	DMN _{TASK}	0.66	0.16	1.15	100	00
	SN-SMN _{MOVIE2}	DMN _{TASK}	0.02	-0.7	0.74	53	23
	VIS _{MOVIE2}	DMN _{TASK}	0.23	-0.34	0.79	80	21
	FPN _{MOVIE2}	DMN _{TASK}	0.04	-0.46	0.54	56	33
	DMN _{MOVIE2}	SN-SMN _{TASK}	0.65	0.31	1.19	100	00
	SN-SMN _{MOVIE2}	SN-SMN _{TASK}	0.07	-0.45	0.59	62	32
	VIS _{MOVIE2}	SN-SMN _{TASK}	0.27	-0.02	0.68	98	07
	FPN _{MOVIE2}	SN-SMN _{TASK}	0.28	-0.06	0.63	95	13
	DMN _{MOVIE2}	VIS _{TASK}	0.2	-0.23	0.67	82	25
	SN-SMN _{MOVIE2}	VIS _{TASK}	-0.15	-0.88	0.57	66	21
	VIS _{MOVIE2}	VIS _{TASK}	0.48	-0.02	1.01	97	5
	FPN _{MOVIE2}	VIS _{TASK}	-0.02	-0.51	0.48	53	34
	DMN _{MOVIE2}	FPN _{TASK}	-0.08	-0.28	0.14	77	55
	SN-SMN _{MOVIE2}	FPN _{TASK}	0.36	0.09	0.64	99	01
	VIS _{MOVIE2}	FPN _{TASK}	-0.16	-0.37	0.05	93	26
	FPN _{MOVIE2}	FPN _{TASK}	0.45	0.25	0.64	100	00

Table S14. Supplementary results from the Bayesian structural equation modelling (BSEM). Direct effects of the relationship between brain CAPs in the “MOVIE2” condition and brain CAPs in the “TASK” condition, neutral context. Median: standardized coefficients of the predictive role for each direct effect. CI_{LOW}-CI_{HIGH}: Range of the ROPE confidence interval (CI 95%). PD: (Probability of Direction) index of effect existence. Significance criterion for the posterior distribution values: <2,5% in ROPE.

INDIRECT EFFECTS AIM2

	CAPS MOVIE2 (X)	REACTION TIME (M)	CAPS TASK (Y)	MEDIAN	CI (LOW)	CI (HIGH)	PD (%)	IN ROPE (%)
NEUTRAL CONTEXT	DMN	RT	DMN	-0.01	-0.2	0.16	56	84
	SN-SMN	RT	DMN	-0.01	-0.22	0.20	56	77
	VIS	RT	DMN	-0.01	-0.18	0.18	55	85
	FPN	RT	DMN	-0.01	-0.2	0.19	55	84
	DMN	RT	SN-SMN	0.05	-0.04	0.32	95	46
	SN-SMN	RT	SN-SMN	0.04	-0.05	0.38	94	38
	VIS	RT	SN-SMN	0.04	-0.15	0.35	9	53
	FPN	RT	SN-SMN	0.04	-0.17	0.37	89	54
	DMN	RT	VIS	-0.04	-0.18	0.10	72	87
	SN-SMN	RT	VIS	-0.03	-0.22	0.12	71	80
	VIS	RT	VIS	-0.03	-0.19	0.10	69	88
	FPN	RT	VIS	-0.03	-0.19	0.12	69	88
	DMN	RT	FPN	0.07	-0.01	0.16	97	76
	SN-SMN	RT	FPN	0.06	-0.17	0.20	69	61
	VIS	RT	FPN	0.07	-0.02	0.18	94	75
	FPN	RT	FPN	0.07	-0.03	0.20	93	74
NEGATIVE CONTEXT	DMN	RT	DMN	0.0	-0.11	0.14	55	96
	SN-SMN	RT	DMN	0.04	-0.32	0.43	6	48
	VIS	RT	DMN	0.01	-0.14	0.18	58	90
	FPN	RT	DMN	0.01	-0.14	0.19	59	88
	DMN	RT	SN-SMN	-0.01	-0.12	0.08	64	98
	SN-SMN	RT	SN-SMN	-0.09	-0.38	0.16	81	50
	VIS	RT	SN-SMN	-0.02	-0.16	0.07	74	91
	FPN	RT	SN-SMN	-0.02	-0.16	0.07	76	90
	DMN	RT	VIS	0.03	-0.1	0.2	67	88
	SN-SMN	RT	VIS	0.17	-0.18	0.57	84	32
	VIS	RT	VIS	0.06	-0.08	0.27	77	77
	FPN	RT	VIS	0.06	-0.08	0.27	79	75
	DMN	RT	FPN	0.05	-0.09	0.18	73	86
	SN-SMN	RT	FPN	0.33	0.10	0.64	1	2
	VIS	RT	FPN	0.09	-0.05	0.21	89	70
	FPN	RT	FPN	0.09	-0.03	0.22	92	67

Table S15. Supplementary results of the Bayesian structural equation modelling (BSEM) mediation analyses. Indirect effects of the relationship between brain CAPs in the “MOVIE2” condition and brain CAPs in the “TASK” condition, mediated by the mean reaction time in the cognitive control tasks. Median: standardized coefficients of the predictive role for each direct effect. CI_{LOW} - CI_{HIGH} : Range of the ROPE confidence interval (CI 95%). PD: (Probability of Direction) index of effect existence. Significance criterion for the posterior distribution values: <2,5% in ROPE.

TOTAL EFFECTS AIM2

	CAPS MOVIE2 (X)	REACTION TIME (M)	CAPS TASK (Y)	MEDIAN	CI (LOW)	CI (HIGH)	PD (%)	IN ROPE (%)
NEUTRAL CONTEXT	DMN	RT	DMN	0.21	-0.1	0.82	77	32
	SN-SMN	RT	DMN	0.07	-0.38	0.54	61	34
	VIS	RT	DMN	0.24	-0.28	0.73	83	20
	FPN	RT	DMN	0.31	-0.28	0.92	86	16
	DMN	RT	SN-SMN	0.3	-0.03	0.75	99	5
	SN-SMN	RT	SN-SMN	0.19	-0.13	0.75	91	15
	VIS	RT	SN-SMN	0.28	-0.1	0.82	94	12
	FPN	RT	SN-SMN	-0.12	-0.61	0.52	55	30
	DMN	RT	VIS	0.14	-0.19	0.46	79	35
	SN-SMN	RT	VIS	0.10	-0.27	0.47	70	39
	VIS	RT	VIS	0.33	-0.06	0.72	95	10
	FPN	RT	VIS	0.21	-0.06	0.9	96	07
	DMN	RT	FPN	0.16	-0.13	0.29	82	19
	SN-SMN	RT	FPN	0.04	-0.08	0.25	81	64
	VIS	RT	FPN	0.16	-0.03	0.36	95	26
	FPN	RT	FPN	0.35	0.15	0.54	100	00
NEGATIVE CONTEXT	DMN	RT	DMN	0.67	0.18	1.18	100	00
	SN-SMN	RT	DMN	0.03	-0.45	0.58	61	31
	VIS	RT	DMN	0.24	-0.31	0.81	81	20
	FPN	RT	DMN	0.24	-0.46	0.58	59	31
	DMN	RT	SN-SMN	0.63	0.28	0.99	100	00
	SN-SMN	RT	SN-SMN	-0.03	-0.41	0.36	57	43
	VIS	RT	SN-SMN	0.24	-0.16	0.64	88	21
	FPN	RT	SN-SMN	0.24	-0.12	0.6	91	19
	DMN	RT	VIS	0.23	-0.23	0.69	84	22
	SN-SMN	RT	VIS	0.02	-0.51	0.53	54	32
	VIS	RT	VIS	0.54	0.02	1.05	100	00
	FPN	RT	VIS	0.04	-0.49	0.55	57	32
	DMN	RT	FPN	-0.03	-0.26	0.19	65	63
	SN-SMN	RT	FPN	0.69	0.36	0.81	100	00
	VIS	RT	FPN	-0.07	-0.32	0.14	79	51
	FPN	RT	FPN	0.54	0.31	0.74	100	00

Table S16. Supplementary results of the Bayesian structural equation modelling (BSEM) mediation analyses. Total effects of the relationship between brain CAPs in the “MOVIE2” condition and brain CAPs in the “TASK” condition, mediated by the mean reaction time in the cognitive control tasks. Median: standardized coefficients of the predictive role for each direct effect. CI_{LOW} - CI_{HIGH} : Range of the ROPE confidence interval (CI 95%). PD: (Probability of Direction) index of effect existence, representing the certainty associated with the most probable direction of the effect. Statistical significance of the posterior distribution values was based on the HDI+ROPE decision rule²⁵ (<2,5% in ROPE).

Supplementary figures

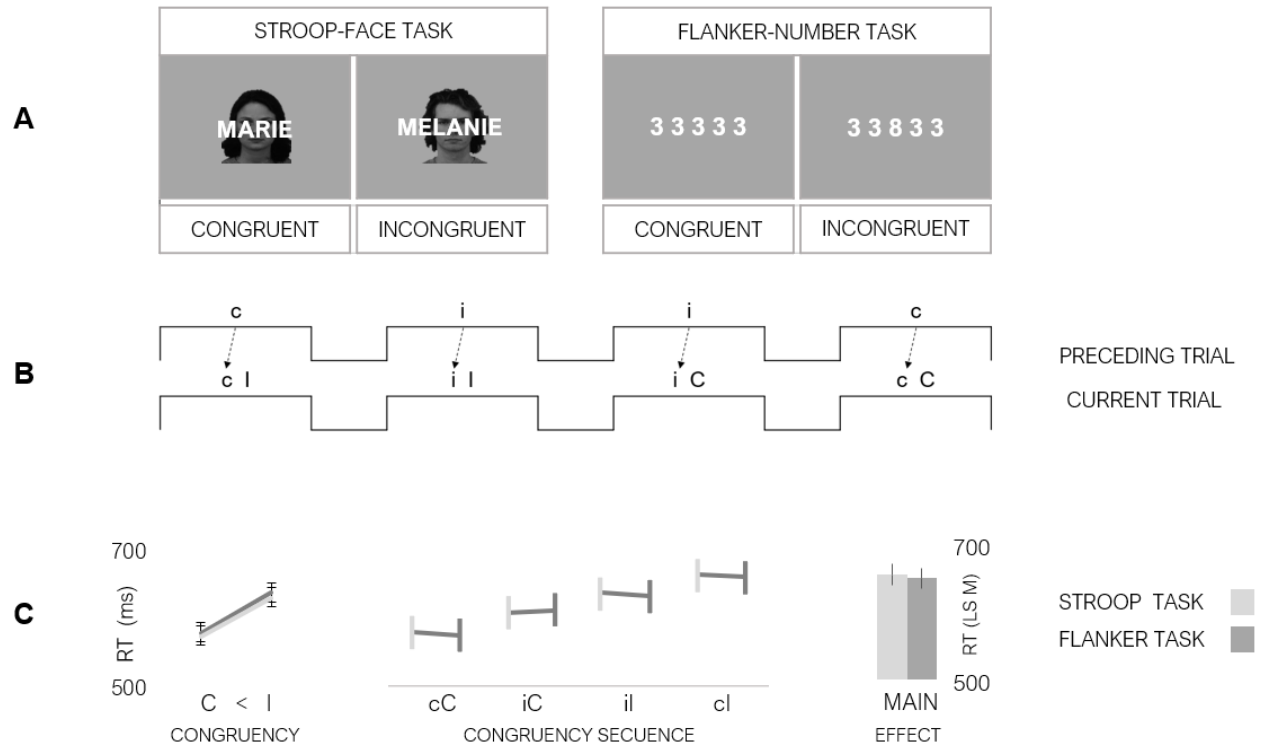


Figure S1. A. Illustration of stimuli in the Stroop task (left) and Flanker task (right). **B.** Trial types in each cognitive task, including congruent (C) and incongruent (I) trials that could be preceded by either the same or opposite condition ("c" or "i" trials), in a semi-random but balanced order. This resulted in 4 experimental conditions, allowing subsequent behavioral analysis according to both current congruence (indicated by upper-case letters "C" and "I") and congruence sequence based on the preceding trial (indicated by lower-case letters "c" and "i"). **C.** Behavioral results from each cognitive control task. Reaction Times across the four trial types showed no significant difference between the two tasks. The interference cost (longer reaction times on incongruent vs congruent trials) was also equally robust in both tasks.

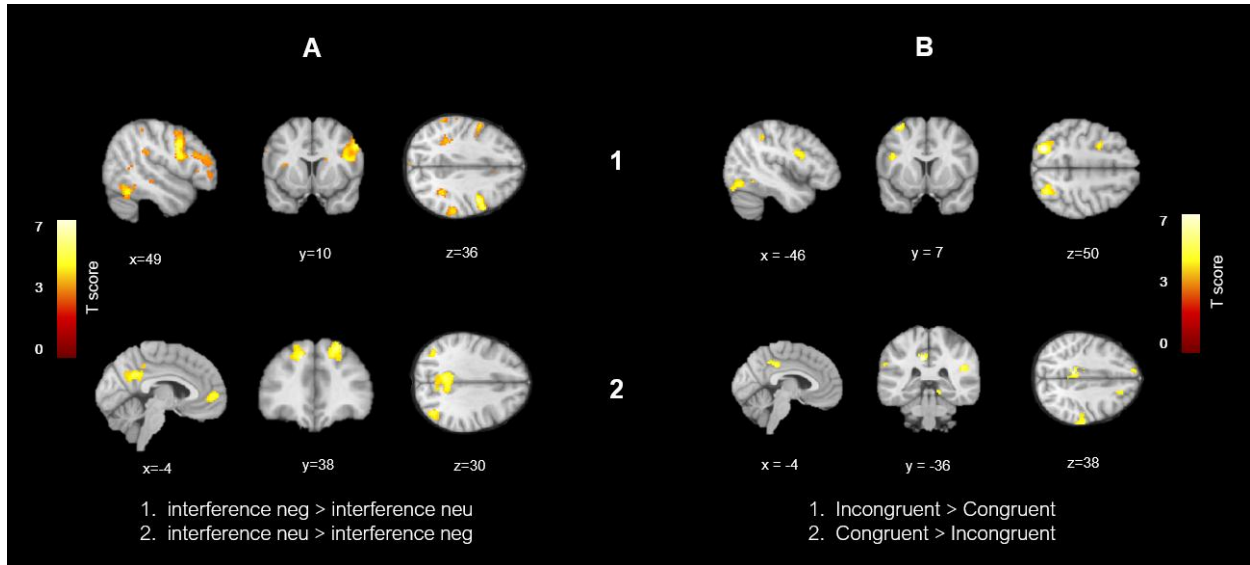


Figure S2. SPM of brain activation showing the main effect of attentional control demands (interference: Inc>Con trials) during the cognitive tasks, pooled across neutral and negative emotion states (**A**), and across the Stroop and Flanker tasks(**B**), and disregarding the affective valence; ($p_{FWE}<.05$ corrected at cluster level. Images displayed at $p_{UNCORRECTED}<.001$; $K>40$).

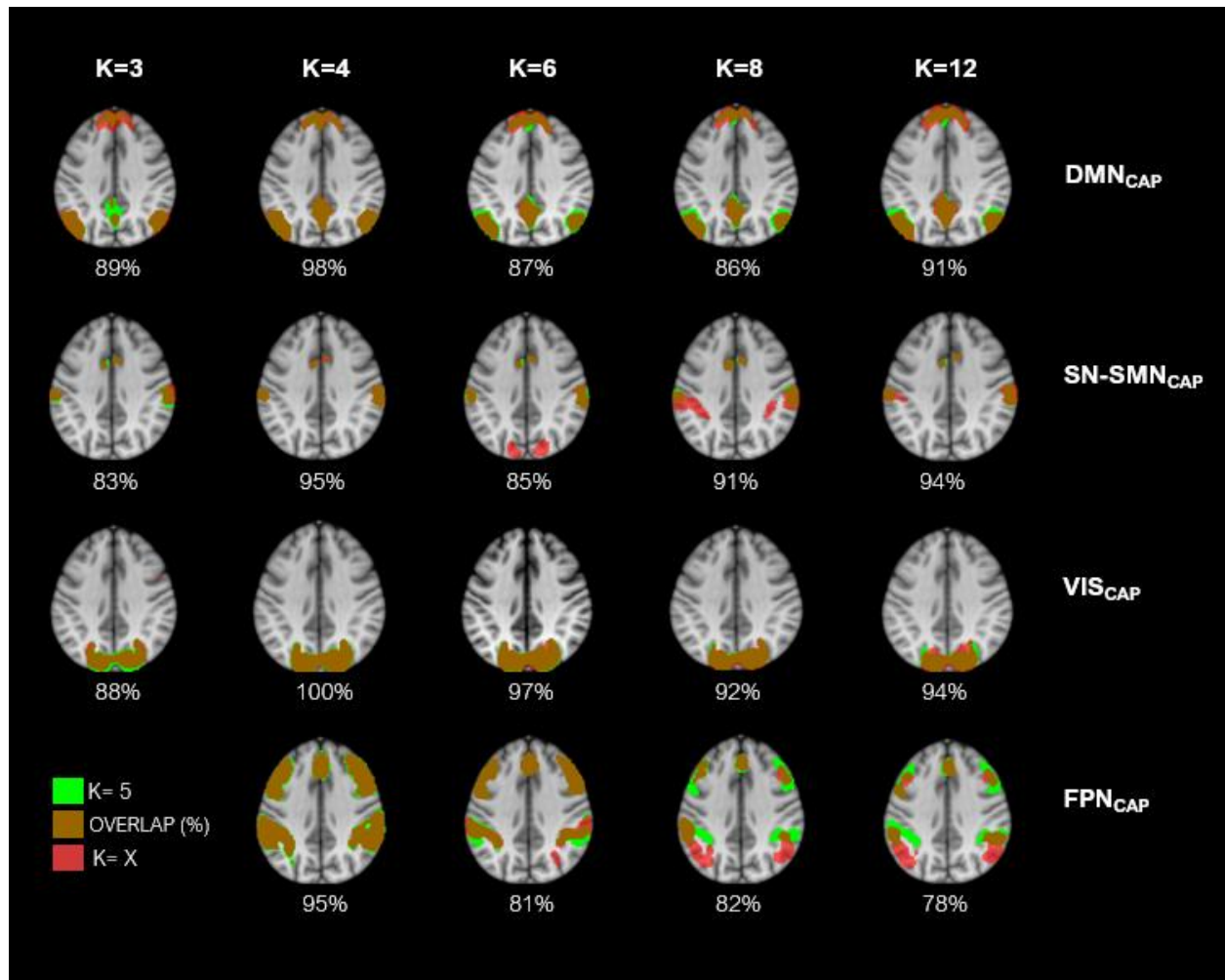


Figure S3. Spatial similarity analysis. Spatial z-maps from different K-mean solutions [$k=3$, $k=4$, $k=6$, $k=8$, $k=12$, displayed in red) were voxel-wise contrasted against a reference clustering ($K=5$, green color). Four maps initially presented the highest overlapping (mean: 90%, brown color) across the considered clustering scenarios. Activation maps were visualized at $z > 1.7$ ($p < .05$).

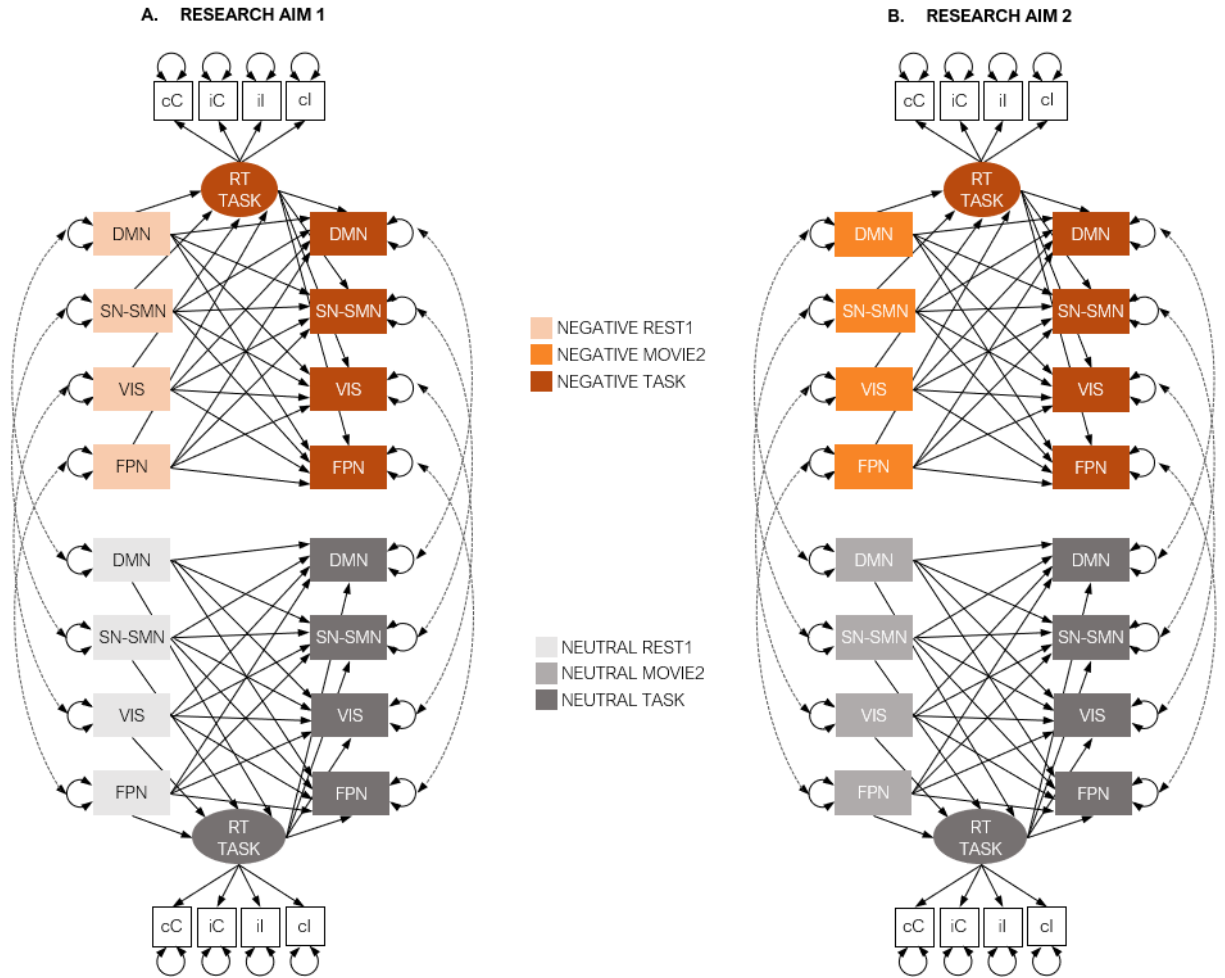


Figure S4. Illustration of BSEMs computed to examine how emotion-induced changes in brain dFC influenced cognitive control. **A.** A first analysis tested the hypothesis that changes in brain activity following the first emotional induction would be apparent in resting state networks (CAPs recorded during the “REST1” condition) and would in turn modify subsequent brain activity patterns recruited during the cognitive control tasks (tasks recorded during the “TASK” condition). Subsequently, a BSEM-based mediation analysis evaluated the influence of the reaction time on the relationships among these brain CAPs. Reaction time (RT) from all types of trials (cC, iC, il, cl) in the cognitive control tasks were also included as factors (squares) of the latent variable “RT TASK” (ovals). **B.** A second set of BSEMs tested the hypothesis that brain dFC patterns evoked by emotional induction itself (CAPs during “MOVIE2” condition) could modify brain networks recruited during cognitive control (CAPs during “TASK” condition). A potential mediation by behavioral data was also assessed. All brain CAPs were modelled individually as manifest variables (rectangles). Double-dashed arrows represent the inter-contexts covariances of individual CAPs. Covariances of CAPs are depicted by double-headed loop arrows. The statistical significance of the posterior distribution values was based on the HDI+ROPE decision rule (<2,5% in ROPE).

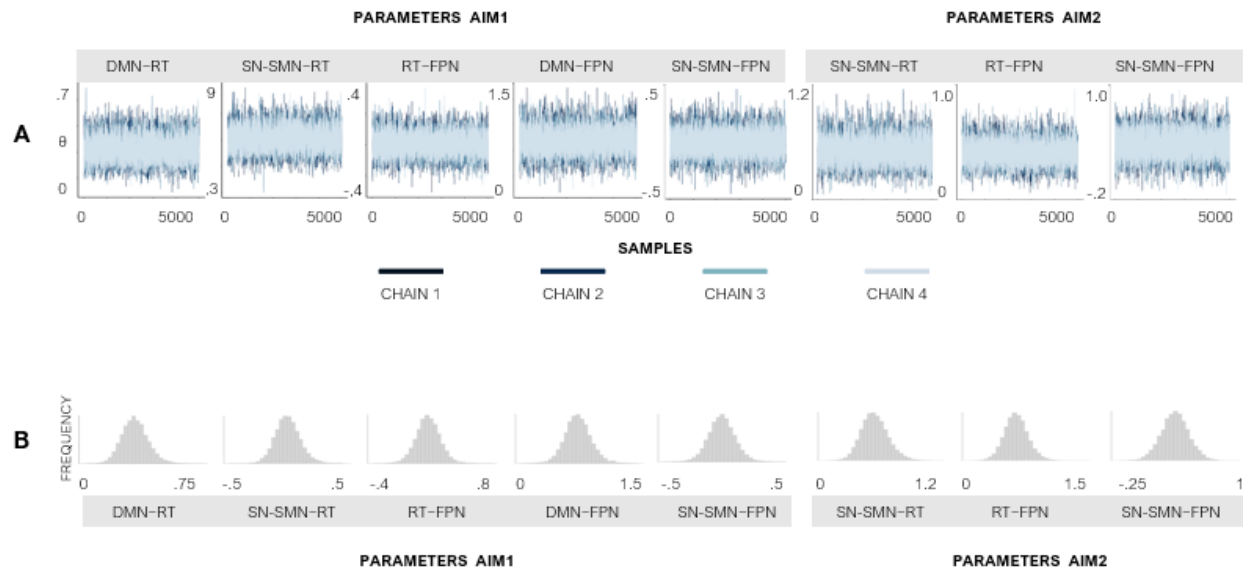


Figure S5. Modelling assessment. **A.** Markov chain plots provided a visual inspection of sampling behavior and mixing across the four chains. **B.** The estimated parameters in the model of AIM1 (left) and the model of AIM2 (right) exhibited smooth densities. The absence of gaps or abnormalities in these distributions confirmed that our models had enough information to represent the posterior distribution in relation to the number of samples. Only parameters with less than 2.5% of the parameter density in the ROPE (see main text for an explanation of this concept) are depicted due to space limitation. The model integrity exhibited by the traceplots and histograms was statistically validated by the PSFR values of the Gelman-Rubin Diagnostic (see list including all the parameters in **Table S10**).

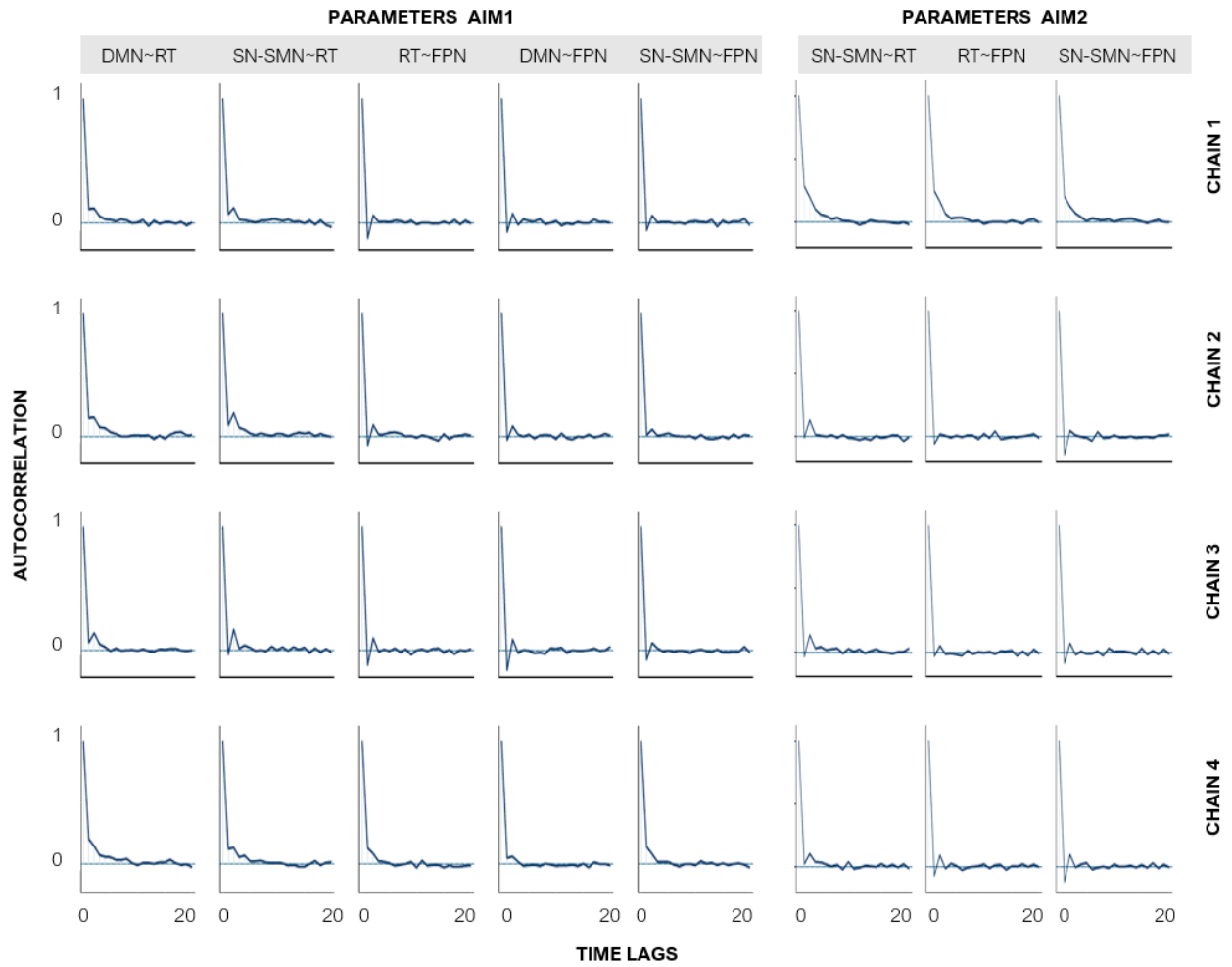


Figure S6. Modelling assessment. Serial autocorrelation plots of significant parameters from the BSEM models [AIM1 (left) and AIM2 (right)]. These parameters presented low serial autocorrelation (i.e., around zero) after the first lag. It denotes a satisfactory number of samples for the estimated parameters.

Supplementary references

1. Gaviria, J. *et al.* Brain functional connectivity dynamics at rest in the aftermath of affective and cognitive challenges. *Hum. Brain Mapp.* **42**, 1054–1069 (2021).
2. Gaviria, J., Rey, G., Bolton, T. A. W., Ville, D. V. D. & Vuilleumier, P. Dynamic functional brain networks underlying the temporal inertia of negative emotions. *NeuroImage* **240**, 118377 (2021).
3. *21 Grams.* . (Universal pictures, USA., 2003). doi:10.1525/fq.2005.58.3.53.
4. *Sophie's Choice.* *World Literature Today* (Twentieth Century Fox Home Entertainment, USA, 1981). doi:10.2307/40135741.
5. Raz, G. *et al.* Portraying emotions at their unfolding: A multilayered approach for probing dynamics of neural networks. *NeuroImage* **60**, 1448–1461 (2012).
6. Raz, G. *et al.* Functional connectivity dynamics during film viewing reveal common networks for different emotional experiences. *Cogn. Affect. Behav. Neurosci.* **16**, 709–723 (2016).
7. Hanich, J., Wagner, V., Shah, M., Jacobsen, T. & Menninghaus, W. Why we like to watch sad films. The pleasure of being moved in aesthetic experiences. *Psychol. Aesthet. Creat. Arts* **8**, 130–143 (2014).
8. Shiota, M. N. & Levenson, R. W. Effects of aging on experimentally instructed detached reappraisal, positive reappraisal, and emotional behavior suppression. *Psychol. Aging* **24**, 890–900 (2009).
9. Borchardt, V. *et al.* Echoes of Affective Stimulation in Brain connectivity Networks. *Cereb. Cortex* **28**, 4365–4378 (2018).
10. Watson, D., Clark, L. A. & Tellegen, A. Development and Validation of Brief Measures of Positive and Negative Affect: The PANAS Scales. *J. Pers. Soc. Psychol.* **54**, 1063–1070 (1988).
11. Bradley, M. & Lang, P. J. Measuring Emotion: The Self-Assessment Semantic Differential Manikin and the. *J. Behav. Ther. Exp. Psychiatry* **25**, 49–59 (1994).
12. Calvo, M. G. & Lundqvist, D. Facial expressions of emotion (KDEF): Identification under different display-duration conditions. *Behav. Res. Methods* **40**, 109–115 (2008).
13. Ashburner, J. *et al.* SPM12 Manual. *Funct. Imaging Lab.* 475–1 (2013) doi:10.1111/j.1365-294X.2006.02813.x.

14. Bolton, T. A. W. *et al.* TbCAPs: A toolbox for co-activation pattern analysis. *NeuroImage* **211**, 116621 (2020).
15. Yan, C.-G., Wang, X.-D. & Lu, B. DPABISurf: data processing & analysis for brain imaging on surface. *Sci. Bull.* **66**, 2453–2455 (2021).
16. Murphy, K. & Fox, M. D. Towards a consensus regarding global signal regression for resting state functional connectivity MRI. *NeuroImage* **154**, 169–173 (2017).
17. Li, M. *et al.* Co-activation patterns across multiple tasks reveal robust anti-correlated functional networks. *NeuroImage* **227**, 117680 (2021).
18. Zhang, J., Huang, Z., Tumati, S. & Northoff, G. Rest-task modulation of fMRI-derived global signal topography is mediated by transient coactivation patterns. *PLoS Biol.* **18**, e3000733 (2020).
19. Liu, X. & Duyn, J. H. Time-varying functional network information extracted from brief instances of spontaneous brain activity. *Proc. Natl. Acad. Sci.* **110**, 4392–4397 (2013).
20. Huang, Z., Zhang, J., Wu, J., Mashour, G. A. & Hudetz, A. G. Temporal circuit of macroscale dynamic brain activity supports human consciousness. *Sci. Adv.* **6**, 1–15 (2020).
21. Power, J. D. *et al.* Methods to detect, characterize, and remove motion artifact in resting state fMRI. *NeuroImage* **84**, 320–341 (2014).
22. Widaman, K. F., Ferrer, E. & Conger, R. D. Factorial Invariance Within Longitudinal Structural Equation Models: Measuring the Same Construct Across Time. *Child Dev. Perspect.* **4**, 10–18 (2010).
23. Dixon, M. L. *et al.* Interactions between the default network and dorsal attention network vary across default subsystems, time, and cognitive states. *NeuroImage* **147**, 632–649 (2017).
24. Cole, M. W. *et al.* Multi-task connectivity reveals flexible hubs for adaptive task control. *Nat. Neurosci.* **16**, 1348–1355 (2013).
25. Kruschke, J. K. Rejecting or Accepting Parameter Values in Bayesian Estimation. *Adv. Methods Pract. Psychol. Sci.* **1**, 270–280 (2018).